Ignition and Combustion of Boron Particles in the Flowfield of a Solid Fuel Ramjet

B. Natan* and A. Ganyt
Technion—Israel Institute of Technology, Haifa, Israel

Theoretical investigation on the behavior of individual boron particles in the flowfield of a solid fuel ramjet (SFRJ) combustor is presented. The study was motivated by the observed difficulties in achieving good combustion efficiencies of boron required to exploit its remarkable theoretical energetic performance. The equations describing the gas flowfield and the particle behavior are solved numerically. The solution presents the trajectory, temperature, and history of the boron particles due to the interactions with the surrounding gas, as well as the ignition envelope and combustion time. The results demonstrate the limited ranges of particle size and ejection velocity which enable ignition and sustained combustion, reveal why practical systems often exhibit poor combustion efficiencies, and predict the conditions where ignition and efficient combustion of boron are feasible.

Nomenclature

A_{for}, A_b = forward and backward reaction kinetics coefficients
A_p = particle cross-sectional area
$\boldsymbol{a}$ = acceleration vector
C_D = drag coefficient
c = parameter defined in Eq. (20)
c_p = specific heat at constant pressure
D = $O_2 - N_2$ diffusivity
d_B = pure boron diameter
d_p = particle diameter
E_{for}, E_b = activation energy of forward and backward reactions
F_D = drag force vector
Fu = fuel
f = fraction of boron in liquid phase
HC = hydrocarbon
ΔH_M = heat of fusion of boron
ΔH_{WR} = heat absorbed by the reaction of H_2O with B_2O_3
ΔH_{VAP} = heat of vaporization of B_2O_3
h = specific enthalpy
$\tilde{h}$ = gas-particle heat transfer coefficient
L_s = effective heat of vaporization or decomposition of the solid fuel
l = Prandtl's mixing length
M = molecular weight
m_p = particle mass
Nu = Nusselt number
P = pressure
Pr = products
$\dot{Q}$ = heat transfer rate to the particle
q_{BR} = heat of boron-oxygen reaction
$\dot{q}_s$ = heat flux to the solid fuel
R_o = universal gas constant
Re = Reynolds number
R_B = molar rate of boron consumption
R_E = molar evaporation rate of boric oxide
R_H = molar rate of removal of boric oxide by water reaction
r = radius; radial coordinate
$\hat{r}$ = radial direction unit vector
$\dot{r}$ = solid fuel regression rate
T = gas temperature
T_p = particle temperature
u = axial velocity
v = radial velocity
$\boldsymbol{w}$ = velocity vector defined in Eq. (14)
X = molar fraction
x = axial coordinate
$\hat{x}$ = axial direction unit vector
Y = mass fraction
δ = oxide layer thickness
ε = particle emissivity
μ = viscosity
ρ = density
σ = Stephan–Boltzman constant
σ_i, σ_h = Prandtl or Schmidt number
$\dot{\omega}$ = rate of chemical reaction
[ ] = molar concentration

Subscripts

B = boron
Bl = boron liquid
ch = chemical
eff = effective
g = gas
h = enthalpy
i = ith chemical component
in = initial
l = laminar
p = particle
s = solid fuel
t = turbulent

Superscript

$\hat{}$ = unit vector

Presented as Paper AIAA 87-2937 at the AIAA/ASEE/ASME/SAE 23rd Joint Propulsion Conference, San Diego, CA, June 29–July 2, 1987; received May 13, 1988; revision received Aug. 13, 1989.

*Currently, National Research Council Postdoctoral Research Associate, Department of Aeronautics, Naval Postgraduate School, Monterey, CA. Senior Member AIAA.

†Associate Professor, Faculty of Aerospace Engineering. Senior Member AIAA.

I. Introduction

THE solid fuel ramjet (SFRJ) seems to be a promising propulsor for a variety of missions, because of its high specific impulse compared to rockets and its relative simplicity compared to other air breathing devices. The addition of certain metals to the commonly used hydrocarbon (HC) fuels can provide even better energetic performance, especially in volume-limited systems.

Boron exhibits remarkable theoretical energetic performance with the highest energy density (i.e., heat release per

unit volume) of all elements, about three times that of HC fuels.[1] However, extracting this theoretical energy is not straightforward. Boron particles are difficult to ignite and to sustain combustion because of a molten oxide layer, which is formed around the particle. This layer serves as a barrier between the oxygen and the boron, thus slowing down the chemical reaction. Besides, prior to their ejection to the flowfield, boron particles tend to coalesce and form relatively large agglomerates whose burning time may be long compared to the residence time in the combustor. Although the ignition and combustion processes of boron have been studied, only a few publications[2,3] have provided information on the particle behavior inside an SFRJ combustor.

The objectives of this study are to analyze and to characterize the behavior of individual boron particles in the flowfield of an SFRJ combustor. An effort is made to explain why in many practical cases the energy release from boron is low compared to the theoretical potential and to demonstrate the conditions in which good combustion efficiencies are feasible.

II. Boron Ignition and Combustion Mechanism

Macek and Semple[4] noted that there are two stages in the boron combustion process. In the first stage (the ignition stage), the particles become luminous, glow for a short period of time, and then tend to extinguish. Under certain conditions, a second and longer stage follows, in which the particles reignite and burn more brightly and completely. The surrounding gas temperature has to be about 1900 K[5] in order to establish the conditions for the second stage (i.e., the sustained combustion).

King[6,7] suggested that the reaction between the boron and the oxygen takes place at the boron-boron oxide interface as a result of oxygen diffusion across the melt layer. This approach was also supported by Safaneev et al.[8] According to the mechanism proposed by Glassman et al.,[9] the reaction occurs at the boron oxide-gas interface as a result of boron diffusion. The latter mechanism was based on evaluation of boron and oxygen solubilities in liquid boron oxide.

The boron-oxygen reaction thickens the oxide layer. On the other hand, it generates heat which, together with heat flux from the gaseous surroundings, increases the particle temperature. As temperature rises, boron oxide evaporates and the thickness of the oxide layer is reduced. This process is endothermic and lowers the rate of particle heating. The presence of water vapor enhances the oxide layer removal by an endothermic water-boron oxide reaction to form gaseous boric acid.[7,10] Ignition occurs when and if the oxide thickness reaches zero.

Both of the oxide production mechanisms[7,9] (Fig. 1) suggest that there is a critical temperature, above which the oxide removal rate exceeds the generation rate. If the particle ignites, the burning rate is mainly controlled by the oxygen diffusion rate through the surrounding gas, although at some finite small particle diameters the burning rate may become kinetically limited.

III. SFRJ Flowfield

The SFRJ combustor can be divided into three major regions (Fig. 2): 1) the head-end region behind the inlet step (approximately 6–7 step heights long), characterized by a separated, recirculation flow; 2) the main region (downstream of the reattachment zone and along most of the fuel grain), where a diffusion flame between the volatile fuel vapors or decomposition products and oxygen is established within the developing boundary layer; and 3) the rear-end region (the aft-mixing-chamber), where there is no fuel grain but where extensive chemical reactions occur because of the good mixing and additional residence time.

The significance of the first region is its essential role in the flameholding process. On the other hand, the second region, which stretches along most of the solid fuel grain, is the main site of the fuel combustion and of the processes leading to the heat-up, ignition, and combustion of boron. Hence, rather than cloud the main issue with a detailed mass of information, it was chosen to focus on this boundary-layer region.

The gas flowfield is assumed to be decoupled from particle influences. However, the thermal, chemical, and dynamic behavior of the individual particles results from their interactions with the surrounding gas flowfield. This behavior is a reasonable description of the situations encountered for low mass fractions of boron in the fuel grain, but may deviate from the actual conditions for highly boron-loaded fuels.

The gas flow is assumed to be steady, turbulent, and of an axisymmetric boundary-layer type. Because the gas-phase combustion process takes place in a diffusion flame zone within the boundary layer, one may assume that the axial diffusion or conduction components are small compared to the radial terms and can be neglected.[11–13] The gas composition is described by concentrations of O_2, N_2, gaseous fuel, water vapor, and other combustion products. The flowfield is described by the following conservation equations:

Continuity:

$$\frac{\partial(\rho_g u_g)}{\partial x}+\frac{1}{r}\frac{\partial(r\rho_g v_g)}{\partial r}=0 \tag{1}$$

Momentum in the axial direction:

$$\rho_g u_g\frac{\partial u_g}{\partial x}+\rho_g v_g\frac{\partial u_g}{\partial r}=-\frac{\partial p}{\partial x}+\frac{1}{r}\frac{\partial}{\partial r}\left(r\mu_{\text{eff}}\frac{\partial u_g}{\partial r}\right) \tag{2}$$

Chemical species:

$$\rho_g u_g\frac{\partial Y_i}{\partial x}+\rho_g v_g\frac{\partial Y_i}{\partial r}=\frac{1}{r}\frac{\partial}{\partial r}\left(\frac{r\mu_{\text{eff}}}{\sigma_{i,\text{eff}}}\frac{\partial Y_i}{\partial r}\right)+\dot{\omega}_i, \qquad i=O_2,N_2,\text{Fu} \tag{3}$$

Energy:

$$\rho_g u_g\frac{\partial h}{\partial x}+\rho_g v_g\frac{\partial h}{\partial r}=\frac{1}{r}\frac{\partial}{\partial r}\left[\frac{r\mu_{\text{eff}}}{\sigma_{h,\text{eff}}}\frac{\partial h}{\partial r}+r\mu_{\text{eff}}\left(1-\frac{1}{\sigma_{h,\text{eff}}}\right)\frac{\partial(u_g^2/2)}{\partial r}\right] \tag{4}$$

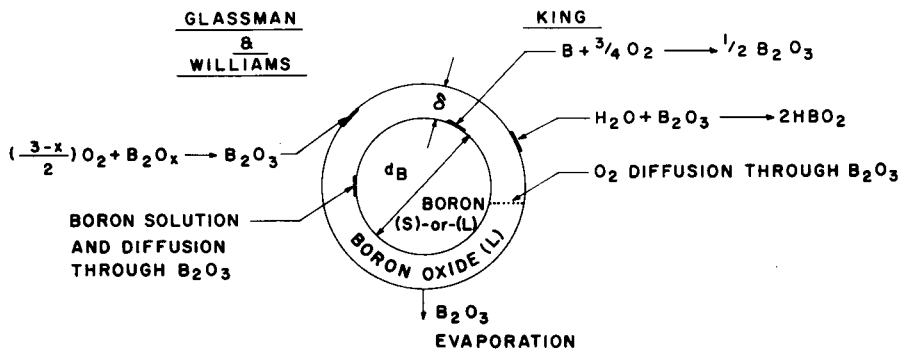

Fig. 1 Proposed ignition mechanisms of a boron particle covered with a thin boron-oxide layer (after Refs. 6 and 9).

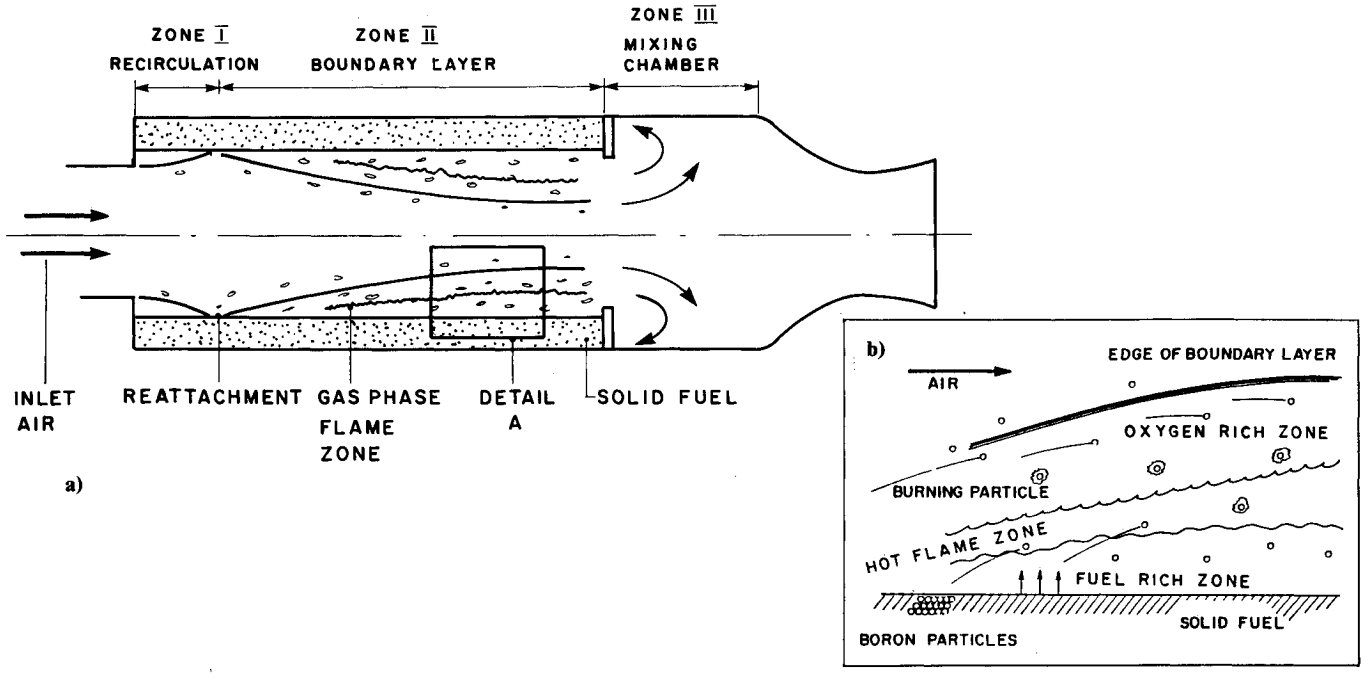

Fig. 2 Flow and combustion features in the SFRJ combustor: a) general view; b) closeup of detail A.

where the stagnation enthalpy is defined as

$$h = c_p T + \frac{u_g^2}{2} + h_{ch} \tag{5}$$

and h_{ch} is the "chemical enthalpy" taking into account the heat of combustion of the fuel.

The effective turbulent transfer coefficients in the above equations are described by Patankar and Spalding.[11] The effective viscosity is taken as the sum of the laminar and turbulent contributions, i.e.,

$$\mu_{\text{eff}} = \mu_l + \mu_t \tag{6}$$

The turbulent viscosity is characterized by the Prandtl mixing length hypothesis:

$$\mu_t = \rho l^2 \left(\frac{\partial u_g}{\partial r}\right) \tag{7}$$

where the mixing length l near the wall is relative to the distance from the wall and reaches a constant value far from the wall.

For the oxidation of the gaseous fuel a global, single step, reversible chemical reaction is used[12,13]:

$$O_2 + \text{Fu} \rightleftarrows \text{Pr} \tag{8}$$

The reaction rate is given by

$$\frac{\text{d[Fu]}}{\text{d}t} = -A_{for} e^{-E_{for}/R_0 T}[\text{Fu}][O_2] + A_b e^{-E_b/R_0 T}[\text{Pr}] \tag{9}$$

The reaction coefficients and activation energies, calculated and adjusted to experimental data by Helman et al.,[12] were used in Eq. (9). The rate of change of the fuel mass per unit volume as the result of the chemical reaction is

$$\dot{\omega}_{\text{Fu}} = M_{\text{Fu}} \frac{\text{d[Fu]}}{\text{d}t} \tag{10}$$

This expression also determines the rate of heat release during the chemical reaction.

The regression rate of the fuel grain is calculated from the heat flux to the wall and the effective heat of gasification of the solid fuel, which includes its sensible heat:

$$\dot{r} = \dot{q}_s / L_s \rho_s \tag{11}$$

On the solid fuel grain surface, the axial velocity and the concentrations of oxygen and products are assumed to vanish. The decomposition and vaporization of the solid fuel is assumed to occur at a temperature of 800 K. On the axis of symmetry, the derivatives of all dependent variables are zero. At the initial cross section of the developing boundary-layer region, profiles of the dependent variables are specified, based on evaluation of the global amount of fuel burned in the recirculation zone.

The boundary-layer-type flowfield was numerically solved by a computer code based on Patankar and Spalding's[11] scheme.

IV. Particle Behavior

After ejection from the condensed fuel into the gas flow, the boron particle motion is dominated by the drag force resulting from the velocity difference between the gas and the particle:

$$\boldsymbol{F}_D = m_p \boldsymbol{a}_p \tag{12}$$

$$\boldsymbol{F}_D = \tfrac{1}{2} \rho_g C_D A_p |\boldsymbol{w}_g - \boldsymbol{w}_p| (\boldsymbol{w}_g - \boldsymbol{w}_p) \tag{13}$$

where

$$\boldsymbol{w} = u\hat{x} + v\hat{r} \tag{14}$$

$$C_D = \frac{24}{Re}(1 + 0.167\, Re^{0.66}) \tag{15}$$

$$Re = \frac{d_p \rho_g}{\mu_g} |\boldsymbol{w}_p - \boldsymbol{w}_g| \tag{16}$$

$$\boldsymbol{a}_p = u_p \frac{\text{d}u_p}{\text{d}x}\hat{x} + u_p \frac{\text{d}v_p}{\text{d}x}\hat{r} \tag{17}$$

Equations (12–17) produce two first-order differential equations for u_p and v_p:

$$u_p \frac{du_p}{dx} - c(u_g - u_p) = 0 \tag{18}$$

$$u_p \frac{dv_p}{dx} - c(v_g - v_p) = 0 \tag{19}$$

where

$$c = \frac{18\mu_g}{d_p^2 \rho_g}(1 + 0.167\, Re^{0.66}) \tag{20}$$

Considering King's[7] model for the ignition stage, the following equations can be written:

$$d_p = d_B + 2\delta \tag{21}$$

$$u_p \frac{dd_B}{dx} = -\frac{2R_B M_B}{\pi d_B^2 \rho_B} \tag{22}$$

$$u_p \frac{d\delta}{dx} = \frac{(R_B/2 - R_E - R_H)M_{B_2O_3}}{\pi d_B^2 \rho_{B_2O_3}} \tag{23}$$

For $T_p < 2450$ K,

$$u_p \frac{dT_p}{dx} = \frac{\dot{Q}}{(\pi/6)d_B^3 c_{p,B}\rho_B + \pi d_B^2 \delta c_{p,B_2O_3}\rho_{B_2O_3}} \tag{24}$$

For $T_p = 2450$ K (boron melting temperature),

$$u_p \frac{df}{dx} = \frac{\dot{Q}}{(\pi/6)d_B^3 \rho \Delta H_M} \tag{25}$$

For $T_p > 2450$ K,

$$u_p \frac{dT_p}{dx} = \frac{\dot{Q}}{(\pi/6)d_B^3 c_{p,Bl}\rho_{Bl} + \pi d_B^2 \delta c_{p,B_2O_3}\rho_{B_2O_3}} \tag{26}$$

$$\dot{Q} = R_B q_{BR} + \pi d_p^2 \bar{h}(T_g - T_p) + \pi d_p^2 \sigma \varepsilon (T_{RAD}^4 - T_p^4) - R_E \Delta H_{VAP} - R_W \Delta H_{WR} \tag{27}$$

$$R_B = 0.16 \times 10^{-12}(d_p^2/\delta) T_p X_{O_2} Pe^{-22{,}600/T_p} \tag{28}$$

$$R_E = \frac{0.32 \times 10^9 \pi d_p^2 Nu T_p^{1/2}}{T_p Nu + 887 Pd_p} e^{-44{,}000/T_p} \tag{29}$$

$$R_H = 4.575 \times 10^{-3} \frac{Nu}{P} d_p T_p^{1/2} \exp\left[18.1\left(1 - \frac{2100}{T_p}\right)\right] \times \left[-0.15 + \left\{0.0225 + 0.987 X_{H_2O} P \times \exp\left[-18.1\left(1 - \frac{2100}{T_p}\right)\right]\right\}^{0.5}\right] \tag{30}$$

The numerical values in the equations correspond to SI units. When and if the oxide thickness reaches zero, the particle ignites (or enters the second stage of combustion), and combustion starts. Assuming that the rate of combustion is controlled by oxygen diffusion to the particle, the molar consumption rate of boron is given by

$$R_B = 2\pi d_p \rho_g (D/M_B) \ell n(1 + 0.677 Y_{O_2}) \tag{31}$$

A special routine was developed to solve the particle behavior, i.e., motion, temperature, and chemical reactions, resulting from the interactions with the surrounding gas.

V. Results and Discussion

Calculations were made for a 2-m-long, 20-cm-i.d. motor, at chamber pressure of 1 MPa (~ 150 psia), and air mass flux of 100 kg/(m²s). For the initial cross section (of the boundary-layer region), the typical velocity profile of a turbulent boundary-layer pipe flow was assumed. The temperature profile consisted of a 1000 K core air temperature, with a narrow 1500 K peak temperature zone at a distance of about one-quarter of the port radius from the wall. The condensed fuel surface temperature was taken as 800 K. The hydrocarbon portion of the solid fuel was represented by the chemical formula CH_2 and an effective heat of vaporization of 300 cal/g.

Characteristic profiles of the gas axial velocity and temperature, mass fractions of O_2 and fuel, and molar fraction of water vapor at a distance of 66 cm from the initial cross section are shown in Fig. 3.

Predictions on boron particle behavior were obtained for particles ejected at a distance of 5 cm from the initial cross section. Initial particle temperature was taken as equal to the wall temperature (800 K). The particle size range relevant to this study is the typical boron agglomerate size upon ejection from the condensed fuel surface.

The main parameters considered in this study were initial particle diameter, ejection velocity and angle, and melt layer (oxide) thickness.

Ignition Characteristics

The particle or agglomerate ejected from the fuel surface enters the flow and is heated by convection and radiation heat transfer. Its trajectory depends on its size, ejection velocity, and ejection angle. As previously mentioned, the particle is covered by a thin, often liquid, boron-oxide layer. The ignition event is characterized by the complete removal of this layer. High surrounding temperatures together with high molar fractions of oxygen and water vapor promote the ignition process of the particle. Obviously, the diffusion flame zone in the boundary layer is the hottest zone in the flowfield. In addition, it contains the highest water vapor fractions due to the reaction between the hydrocarbon fuel and the oxygen. Thus, it seems logical that a long residence time in this zone promotes ignition.

The ignition behavior of various size boron particles is presented in Fig. 4. If the ejection velocity component vertical to the fuel surface is small, the particle rolls over the fuel surface where the temperature is not sufficiently high and the amounts of oxygen and water vapor are limited; hence, ignition does not occur. At a certain vertical ejection velocity the particle may ignite, although ignition time is long. An increased ejection velocity brings the particle closer to the flame zone, thus reducing the ignition time, until it reaches a minimum value. A further increase in the vertical ejection

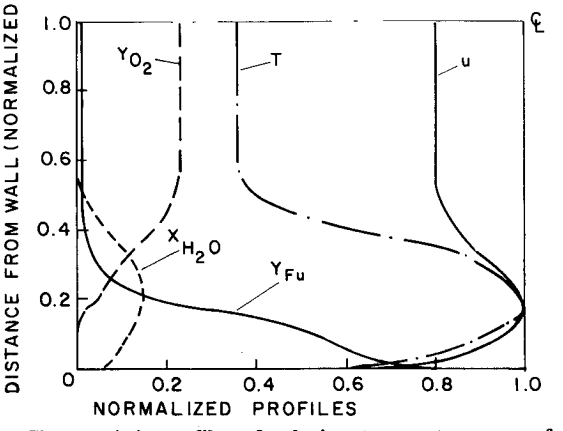

Fig. 3 Characteristic profiles of velocity, temperature, mass fractions of O_2 and fuel, and molar fraction of water vapor.

velocity shortens the residence time in the hot flame zone and shoots the particle towards the cooler zone above the flame. This causes the ignition time to increase with ejection velocity. An increase of the ejection velocity above a certain value results in a failure of the particle to ignite. The range of ejection velocities for which ignition of the particles can be obtained is affected by the particle size. Because of their inertia, larger particles need lower ejection velocities to reach the same distance from the surface.

Effect of Initial Boron-Oxide Thickness

Figure 5 presents the ignition time of a 25-μ particle vs the ejection velocity for two values of initial oxide-layer thickness, 0.1 and 0.2 μ. There is only a slight effect of the oxide-layer thickness, indicating that the heating process dominates the overall ignition time. When the particle temperature exceeds approximately 1900 K, the oxide removal is rather fast.

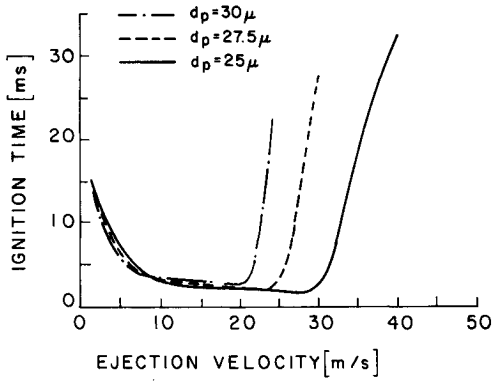

Fig. 4 Effect of ejection velocity on ignition time.

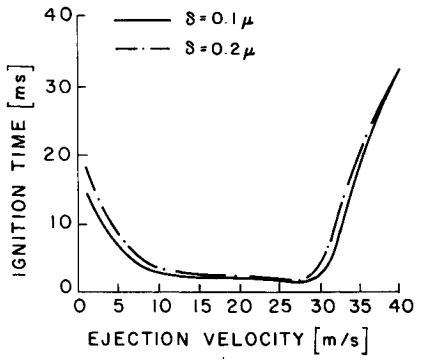

Fig. 5 Effect of initial boron-oxide thickness on ignition time, $d_{p,in} = 25\ \mu$.

Ejection-Angle Effect

Particles are ejected in all directions.[2,3] The ejection angle combined with the ejection velocity affects the ignition time through its influence on the particle trajectory and the residence time in the hot flame zone. Figure 6 presents the ignition time of 25-μ boron particles ejected at various ejection angles. The ejection angle is measured from the downstream direction of the fuel surface. Ejection angle of 90 deg represents direction vertical to the fuel surface.

Particle Ignition Zone

The ejection velocity and angle of a particle of certain size was found to determine its ignition location. The geometric locus of all ignition locations of the same particle can be defined as the ignition zone and is described in Fig. 7. The physical significance of the ignition zone is that particles whose trajectories cross the boundaries of this zone do ignite, while those that miss this ignition envelope do not ignite. The ignition zone lies downstream of the particle ejection point. For larger particles this zone moves further downstream, but remains basically similar. One can conclude that most regular-size boron particles, whose ejection velocities are not too extreme, are likely to ignite.

Combustion Characteristics

Burning times (including ignition and complete combustion) were calculated for boron particles as a function of the ejection velocity. A 0.1-μ-thick boron oxide layer and perpendicular ejection were assumed. The results shown in Fig. 8 demonstrate that there is a limited range of ejection velocities which produce ignition and complete combustion of the particle. The boundaries of this range shrink for larger particles.

It should be noted that ignition, defined by complete removal of the oxide layer, does not guarantee sustained com-

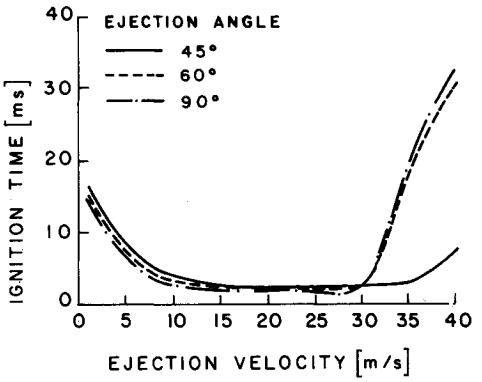

Fig. 6 Effect of particle ejection angle on ignition time, $d_{p,in} = 25\ \mu$.

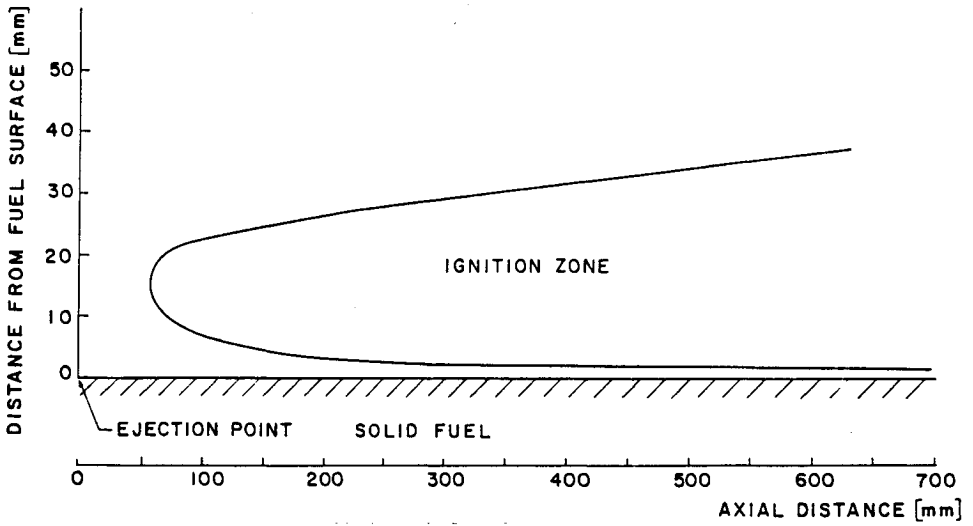

Fig. 7 Particle ignition zone within the combustor flowfield with respect to the ejection point.

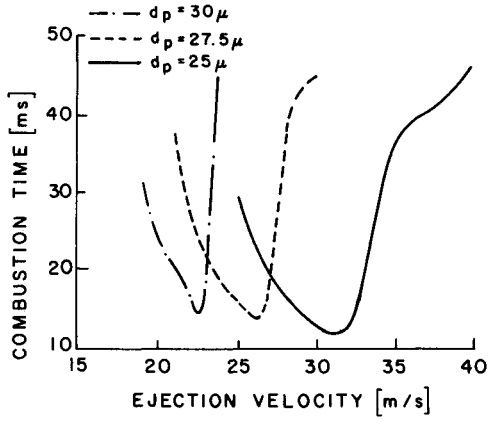

Fig. 8 Effect of particle size on the overall combustion time.

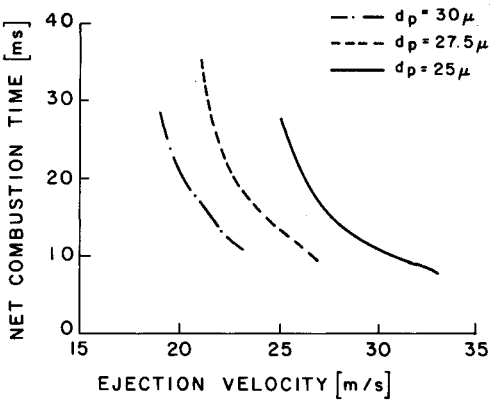

Fig. 9 Net combustion time vs ejection velocity.

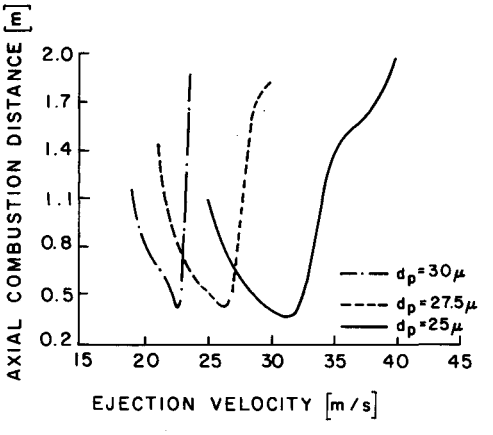

Fig. 10 Effect of ejection velocity on the axial distance for complete combustion.

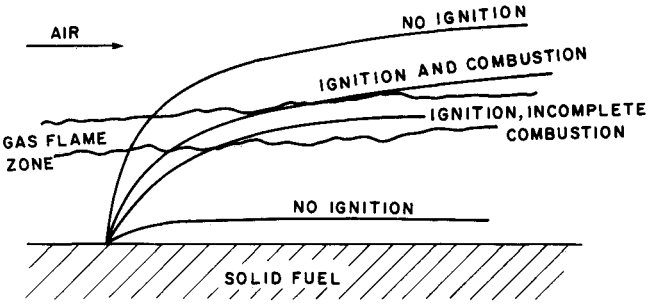

Fig. 11 Schematic description of ignition and combustion characteristics of boron particles having different trajectories.

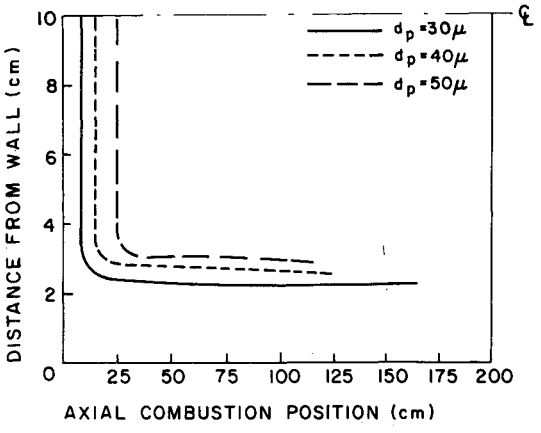

Fig. 12 Axial distance for complete combustion of already-ignited particles dispersed at various distances from the fuel surface.

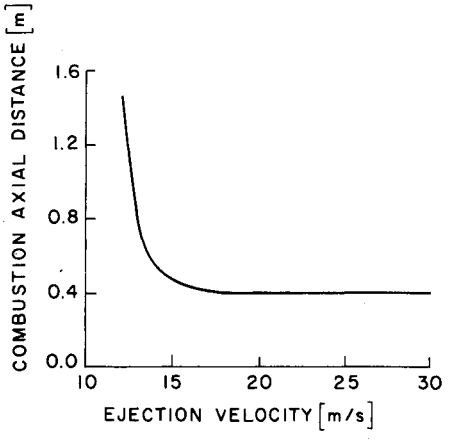

Fig. 13 Axial distance for complete combustion of preheated particles vs ejection velocity, $d_{p,in} = 50\ \mu$, $T_{p,in} = 2000$ K.

bustion of the particle. The ignition zone is close to the gas-phase flame zone, and stretches mainly below it (towards the wall), where the oxygen concentration is relatively low. Ignition in such situations may result in very low reaction rates that may lead to extinguishment, which may be the case for low ejection velocities.

An increase in ejection velocity enables ignition and combustion. Minimum combustion time is achieved at certain ejection velocities. A further increase in ejection velocity increases the ignition delay, hence increases the total combustion time. In general, the net combustion time (measured from the ignition event to the completion of combustion) decreases with increasing the ejection velocity (Fig. 9). Higher ejection velocities, although causing longer ignition delays, enable the particle to achieve greater distances from the surface, where the oxygen concentration is higher, thus they reduce the net combustion time.

The major concern is whether or not a particle ejected from the wall can burn completely inside the motor. Calculations show that small particles (up to 30 μ) need to travel at least 1 m inside the motor for complete combustion. Larger particles, even if they ignite, may not burn completely even after 2 m. The axial combustion distance as a function of the ejection velocity, for various small-size particles ejected perpendicular to the surface, is presented in Fig. 10. The shapes of the curves are similar to those of Fig. 8. Figure 11 is a schematic summary of the ignition and combustion characteristics of particles having different trajectories demonstrating the sensitivity of the overall combustion process to parameters of limited control.

In order to characterize the combustion itself, isolated from the ignition phenomena, the behavior of already ignited

boron particles, dispersed at the initial cross section, was analyzed. Such a situation may be encountered in real boron-rich SFRJ combustors, where particles originating in the recirculation zone enter the main combustor section already ignited. Axial distances for complete combustion of particles of 30, 40, and 50 μ dispersed at different distances from the fuel surface are presented in Fig. 12. It can be seen again that particles which move along the centerline region burn faster than those whose trajectories are closer to the fuel surface. Ignition in an oxygen-rich zone enables even relatively large particles (50-μ diameter) to complete their burning within a short distance from their initial point. Particles of similar sizes that are ejected from the fuel surface can scarcely ignite and burn.

The interesting result, that complete combustion of boron particles is possible once the necessary conditions for igniting and situating the particle in an oxygen-rich zone are fulfilled, indicates a direction for achieving efficient combustion. The crucial stage of ignition may be overcome by preheating the particles upon their ejection from the fuel surface. Calculations made for 50-μ-diam particles ejected at an initial temperature of 2000 K at various velocities reveal a remarkable decrease in burning time and distance for complete combustion (Fig. 13) compared with particles ejected at the regular wall temperature (800 K).

VI. Conclusions

The study reveals that the general flowfield characteristics of the SFRJ combustor are inherently unfavorable for the combustion of boron particles ejected from the solid fuel. The requirements for boron ignition, particularly high surrounding temperatures, are often associated with the low oxygen content, gas-phase reaction zone. Boron combustion, on the other hand, requires high oxygen fractions. This is the reason why only particles of very specific characteristics (size and ejection velocity and angle) are predicted to burn efficiently inside the combustor. As a conclusion, the overall combustion efficiency of an SFRJ combustor is predicted to be generally low, in accordance with available experimental findings.

It is, however, indicated that efficient combustion may be expected by either preheating the particles before leaving the surface, thus saving the initial ignition stage, or by situating the already ignited particles in a high-oxygen-concentration zone.

References

[1]Gany, A., and Netzer, D. W., "Fuel Performance Evaluation for the Solid-Fueled Ramjet," *International Journal of Turbo and Jet Engines*, Vol. 2, No. 2, 1985, pp. 157–168.

[2]Gany, A., and Netzer, D. W., "Combustion Studies of Metallized Fuels for Solid-Fuel Ramjets," *Journal of Propulsion and Power*, Vol. 2, No. 5, 1986, pp. 423–427.

[3]Scott, C. K., II, and Netzer, D. W., "Metallized Fuel Burning Characteristics in the Solid Fuel Ramjet," 23rd JANNAF Combustion Meeting, CPIA Pub. 457, Chemical Propulsion Information Agency, Johns Hopkins University, Laurel, MD, Vol. 1, 1986, pp. 353–364.

[4]Macek, A., and Semple, J. M., "Combustion of Boron Particles at Atmospheric Pressure," *Combustion Science and Technology*, Vol. 1, 1969, pp. 181–191.

[5]Faeth, J., "Status of Boron Combustion Research," Air Force Office of Scientific Research, Washington, DC, AFOSR/NA Rept., Oct. 1984.

[6]King, M. K., "Ignition and Combustion of Boron Particles and Clouds," *Journal of Spacecraft and Rockets*, Vol. 19, No. 4, 1982, pp. 294–306.

[7]King, M. K., "Boron Particle Ignition in Hot Gas Streams," *Combustion Science and Technology*, Vol. 8, No. 4, 1974, pp. 243–255.

[8]Safaneev, D. Z., Kashporov, L. Ya., and Grigorev, Yu. M., "Heat-Liberation Kinetics in Boron-Oxygen Interaction," *Combustion, Explosion, and Shock Waves*, Vol. 17, No. 2, 1981, pp. 210–214.

[9]Glassman, I., Williams, F. A., and Antaki, P., "A Physical and Chemical Interpretation of Boron Particle Combustions" 20th Symposium (International) on Combustion, Combustion Inst., Pittsburgh, PA, 1984, pp. 2057–2064.

[10]Gaponeko, L. A., Biunoivskii, S. N., Tulupov, Yu. I., and Yakovleva, T. A., "A Model for the Ignition of a Single Boron Particle in a Medium-Containing Water," *Combustion, Explosion, and Shock Waves*, Vol. 17, No. 1, 1981, pp. 9–14.

[11]Patankar, S. V., and Spalding, D. B., *Heat and Mass Transfer in Boundary Layers*, 2nd ed., Intertext Books, London, 1970.

[12]Helman, D., Wolfshtein, M., and Timnat, Y. M., "Theoretical Investigation of Hybrid Rocket Combustion by Numerical Methods," *Combustion and Flame*, Vol. 22, No. 2, 1974, pp. 171–190.

[13]Gany, A., Timnat, Y. M., and Wolfshtein, M., "Two-Phase Flow Effects on Hybrid Combustion," *Acta Astronautica*, Vol. 3, No. 3–4, 1976, pp. 241–263.